Chiang Mai J. Sci. 2017; 44(3) : 1100-1112
http://epg.science.cmu.ac.th/ejournal/
Contributed Paper

Effect of Vibro-milling Time on Phase Transformation and Particle Size of Zirconia Nanopowders Derived from Dental Zirconia-based Pre-sinter Block Debris

Chana Sriboonpeng [a,c], Jeeranan Nonkumwong [b,c], Laongnuan Srisombat [b] and Supon Ananta* [a]

[a] Department of Physics and Materials Science, Faculty of Science, Chiang Mai University, Chiang Mai 50200, Thailand.

[b] Department of Chemistry, Faculty of Science, Chiang Mai University, Chiang Mai 50200, Thailand.

[c] The Graduate School, Chiang Mai University, Chiang Mai 50200, Thailand.

* Author for correspondence; e-mail: suponananta@yahoo.com

Received: 11 December 2016
Accepted: 11 January 2017

ABSTRACT

Zirconia (ZrO_2) nanopowders (with smallest size ~ 35 nm) derived from recycling of dental ZrO_2-based pre-sinter block debris were prepared by using a rapid vibro-milling technique. The detailed investigations considering the roles of vibro-milling times on crystal structure, particle size distribution and morphological evolution of the obtained powders were investigated by using a combination of X-ray diffraction (XRD), laser diffraction, scanning electron microscopy (SEM) and transmission electron microscopy (TEM) techniques. In general, it has been found that the monoclinic- and the tetragonal-ZrO_2 phases tend to form together. The increased milling time was found to play a significant role on broadening of particle size distribution together with fluctuation of ZrO_2 particle size. Moreover, SEM results showed that these ZrO_2 powders consist of a variety of agglomerated particle size, depending on their experienced vibro-milling times. In addition, TEM technique was also used to confirm the crystallographic phases of the ZrO_2 nanoparticle supporting the XRD results. These findings revealed that a narrower particle size distribution of these ZrO_2 nanopowders can be tailored by employing an appropriate choice of the milling time.

Keywords: zirconia, nanopowders, recycling wasted dental debris, vibro-milling

1. INTRODUCTION

Partially stabilized zirconia is one of the significant restorative materials for dental applications owing to their suitable biocompatibility, wear resistance and high mechanical properties [1, 2]. Therefore, it has been employed extensively for dental restoratives, such as crowns, bridges, implant fixtures and implant abutments due to its suitable properties for dental prostheses [2, 3]. In recently, the fabrication of dental materials using dental ZrO_2-based pre-sinter blocks has been performed by using

Computer Aided Design/Computer Aided Manufacturing (CAD/CAM) technology with machining [4]. CAD is used to scan crown or bridge models three-dimensionally. Then, the collected scanning data is transferred to CAM unit to fabricate the prostheses products [4]. During these experienced CAD/CAM procedures, major debris of the milled ZrO_2-based pre-sinter block are generated as wasted powders [5]. As is well-known, the waste materials from factories increase every year, one of the key issues regarding environmental damage attributed by several industrial productive sectors was the discharge of unwanted materials directly into ecosystems without a good treatment [5-7]. As a consequence, if the dental industries carefully focus on recycling waste debris as the potential options, the environmental problems could be minimized in a manageable way. Hence, low-cost alternative method to recycle these wastes should open new window for the future and this matter is also challenging for both the academic and the manufacturing points of view. We are therefore interested in the elevation of dental ZrO_2-based pre-sinter block debris into nanopowders in order to gain better opportunity such as reducing waste, producing added-value ZrO_2 raw materials which can be used for the fabrication of high packing density and uniform microstructure of the sintered ceramic body for forming dental prostheses via CAD/CAM machining or other ZrO_2-related products [8].

To date, several kinds of advanced ceramics available for medical and dental applications are being manufactured from nanoparticles which can be successfully prepared via various mechanical milling methods [9-11]. Although the conventional ball-milling technology is stable and readily available due to its energy efficiency, the vibro-milling which is a vibrating vessel machine containing cylindrical grinding media at amplitudes up to approximately 5 cm seems to be more attractive [9, 10]. Based on the original work performed on several kinds of nanopowders, it is observed that relative to ball-milling, vibro-milling produces finer particles and a narrower size distribution at a faster rate [9, 10]. This implies that fine grinders like a vibro-mill are addressed as a tool for producing nanopowders, and the milling time is a key parameter for such materials processing as well as the nanopowder preparation [9, 10]. Alternatively, the advantage of using a mechanical milling for preparation of nanopowders comes from its capability to produce mass quantities of nanopowders within a short time using simple equipment and low-cost starting precursors, applicable to any class of materials [9-11]. In this connection, the effect of milling time on phase formation and particle size of ZrO_2 nanopowders was investigated. Moreover, to the best of our knowledge, this is the first study to consider the role of vibro-milling technique together with their optimal milling conditions as the potential recycling process for the production of ZrO_2 nanopowders from waste dental ZrO_2-based pre-sinter block debris. Important questions such as how long the vibro-milling takes to produce the possible smallest particles, how broad the particle size distribution and how these characteristics depend on the milling time will be addressed.

2. MATERIALS AND METHODS

Dental ZrO_2-based pre-sinter block debris was collected in vacuum system after the daily machining of prostheses from a dental laboratory using a CAD/CAM system. As-received powders were first cleaned with deionized water and then dried at 120 °C for 24 h in an oven to remove dust,

any possible contamination and water content in waste ZrO_2 powders. Preliminary investigation on these dental ZrO_2-based pre-sinter block powders was carried out via several techniques including XRD, laser diffraction, SEM and TEM techniques.

In order to investigate the effect of milling time on phase formation and particle size of these dental ZrO_2 powders, a vibratory laboratory mill powered by a 1/30 HP motor [9, 10] was performed. The grinding vessel consists of a 125 ml capacity polypropylene jar fitted with a screw-capped, gasket less, polyethylene closure. The jar is filled with an ordered array of identical and cylindrical grinding media of ZrO_2. A total of 48 milling media cylindrical with a powder weight of 20 g were kept constant in each batch. The milling operation was performed with various milling times ranging from 0.5-10 h in ethanol inert to the polypropylene jar [9, 10]. Drying was carried out at 120 °C for 24 h to remove ethanol from each batch of ZrO_2 powders.

All powders were characterized by room temperature XRD (Rigaku, MiniFlex II) using Ni-filtered Cu-K_α radiation (λ = 1.5406 Å), to identify phase formation and the optimal milling time for the production of ZrO_2 powders having the smallest size. The average crystallite size was also calculated via Scherrer's equation [12]. The tetragonal (t) (111) reflection at $2\theta \sim 30.1°$ was used to define full width at half-maximum intensity (FWHM). The lattice strain was estimated from broadening XRD peaks by Williamson-Hall formula [13]. The particle size distributions of the powders were determined by laser diffraction techniques (Mastersizer S, Malvern Instruments Limited). The morphological evolution of the powders was observed by SEM (JEOL JSM-6335F) and TEM (JEOL JEM-2010) where powder samples were dispersed in ethanol and deposited by pipette onto 3 mm holey copper grids. The corresponding crystal structures of the observed phases were then evaluated by correcting the XRD and TEM diffraction data.

3. RESULTS AND DISCUSSION

Apart from the applications of ZrO_2-based ceramics itself, it is well-documented that ZrO_2 particles with metastable tetragonal phase have normally been used as a dispersed phase in a number of advanced ceramics to enhance their mechanical properties (e.g. tensile strength, wear resistance and fracture toughness) [1-3]. As demonstrated by a number of publications [14-16], the tetragonal form of ZrO_2 was stabilized by the excess surface energy of the fine grains of ZrO_2 when the surface energy of the tetragonal form is smaller than that of the monoclinic form. However, under the influence of stress induced and associated with a reduction in average crystallite size, the tetragonal ZrO_2 phase transforms into the monoclinic ZrO_2 phase. This ZrO_2 transformation also occurred by gentle milling [17], vibration ball-milling [16] and ultrasonic treatment [18]. Therefore, to further examine the influence of different vibro-milling time on phase formation of dental ZrO_2-based pre-sinter block powders, XRD technique was employed. The XRD results in Figure 1 indicate that all samples show (t) ZrO_2 phase with lattice constants a = 5.12 pm and c = 5.25 pm (corresponding to JCPDS file number 17-0923) as a major phase which is stable at room temperature and (m) ZrO_2 with lattice constants a = 5.312 pm, b = 5.212 pm, c = 5.147 pm and β = 99.128° (corresponding to JCPDS file number 37-1484) as a minor phase, where no additional peaks corresponding to any new phase were observed up to 10 h of milling, consistent with those observed by Adam *et al.* [19]. This is clear from the data

collected in the 2θ range of 27-34°, within which the main peaks of all ZrO_2 polymorphs must appear, as shown in Figure 2. All of them clearly reveal the intensity changes observed from m ($\bar{1}11$) and m (111) peaks when the intensities of t (111) peak for all samples were adjusted into the same level.

The amount of (m) ZrO_2 phase in each vibro-milled powder may, in principle, be estimated from the intensities of the most intense X-ray reflections for the (t) and (m) phases by employing the following equation:

$$\text{wt.\% monoclinic phase} = \left(\frac{I_{m(\bar{1}11)}}{I_{t(111)} + I_{m(\bar{1}11)}} \right) \quad (1)$$

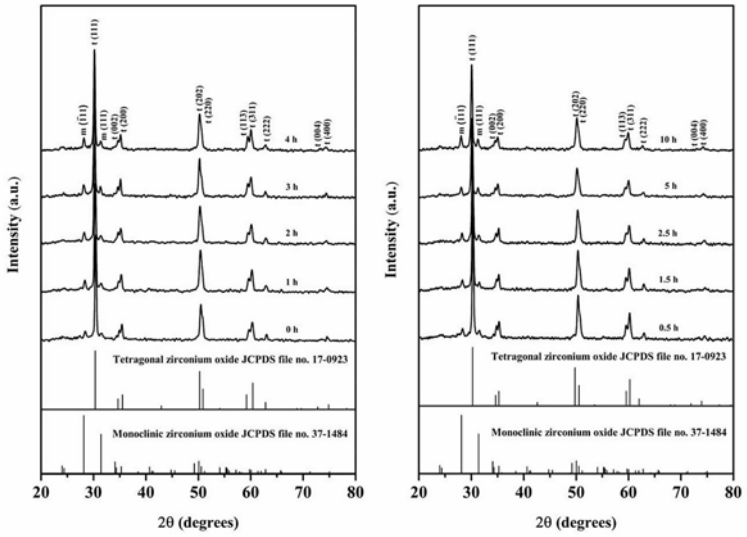

Figure 1. XRD patterns of waste ZrO_2 powders milled for various time.

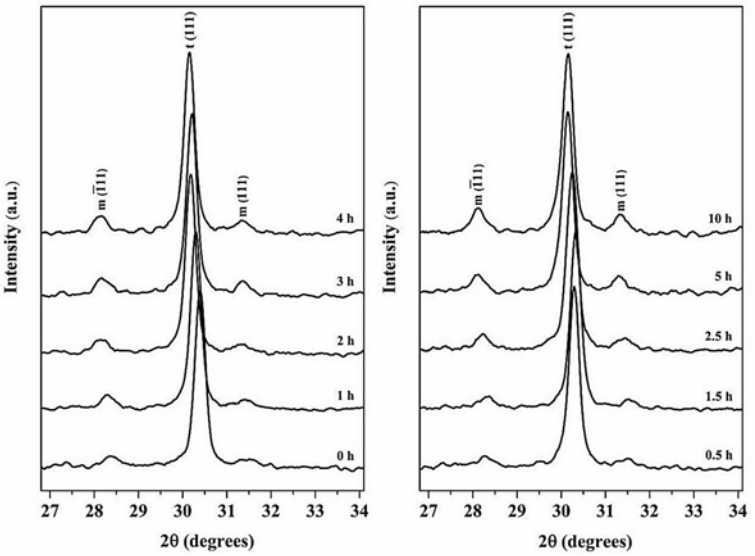

Figure 2. Enlarged zone of Figure 1 showing the relative ratios of the t (111) m ($\bar{1}11$) and m (111) peaks as a function of milling time.

This equation should be seen as a first approximation since its applicability requires comparable maximum absolute intensities of the pair of (t) and (m) ZrO_2 peaks being used [20, 21]. Here I_m and I_t refer to the intensities of m ($\bar{1}11$) and t (111) peaks, respectively. This equation is analogous to the well-known equation widely employed in connection with the fabrication of other ceramic materials [20, 22]. On the other hand, if the expected ratio between the intensities of the two monoclinic peaks (*i.e.* m ($\bar{1}11$) and m (111)) is known and the intensity of m (111) peak can be accurately determined [23, 24], then the integrated intensity ratio (X_m) is also used apart from eq. (1) and is defined as:

$$X_m = \frac{I_{m(\bar{1}11)} + I_{m(111)}}{I_{m(\bar{1}11)} + I_{m(111)} + I_{t(111)}} \qquad (2)$$

where the subscripts *m* and *t* refer to the monoclinic and tetragonal phases, respectively and $I_{(hkl)}$ implies the integrated intensity of the diffraction line indicated by its Miller indices. Eq. (2) was originally intended to identify the fraction of (m) phase in a polymorphic mix of ZrO_2 by establishing linear calibration curves for X_m as a function of the actual weight fraction of monoclinic. However, a linear intensity concentration relationship is based on the assumption that the intensities of $I_{t(111)}$ peak are equal to sum of the (m) peaks $I_{m(\bar{1}11)} + I_{m(111)}$, which are not strictly correct [24]. In order to determine the relative contents of the phases present, eqs. (1) and (2) have been applied to these powder XRD patterns. The results for the two equations are compared (in Table 1) as a function of milling time. This study shows that both equations provided comparable results that the qualitative concentrations of (m) ZrO_2 phase tend to increase significantly but the qualitative concentrations of (t) ZrO_2 phase tend to decrease when longer milling times were applied. However, there was some difference between these two data sets at 0 h milling which the calculated ZrO_2 content derived from eq. (2) is almost 2-times higher than that from eq. (1). This might be due mainly to an error from the measurement of the integrated intensities of partially overlapping m (111) and t (111) reflections [23] or an unequal $I_{t(111)}$ to the sum of $I_{m(\bar{1}11)}$ and $I_{m(111)}$ as mentioned earlier [24]. Therefore, the calculated ZrO_2 contents from eq. (1) will henceforth be considered. At 0 h milling, *i.e.* as-received dental ZrO_2-based pre-sinter block debris, there was few (m) ZrO_2 phase among (t) ZrO_2 phase. This could be due to the martensitic (t) to (m) phase transformation induced by mechanical stress during CAD/CAM process. To support this idea, the ZrO_2 powders were milled with elongated milling times. The results (Table 1) show that the calculated monoclinic content is likely to be independent of milling time from 0 to 3 h. It means that milling for 0.5 h to 3 h may not provide enough energy for more transformation of (t) ZrO_2 [25]. By increasing the milling time more than 3 h, the results show that the amount of (m) ZrO_2 continuously increases. This observation demonstrated that the metastable (t) phase can be transformed into the (m) phase during the prolonged milling due to influence of the produced stress. Based on the obtained XRD data, it may be stated that (t) to (m) phase transformation would generate stresses and strains to be included in the structure that might cause the particle fracture. This finding is in agreement with earlier work reported by Shukla *et al.* [26].

Table 1. Calculated ZrO_2 phase as a function of milling time.

Milling time (h)	Qualitative concentrations of ZrO_2 phase calculated by eq. (1)		Qualitative concentrations of ZrO_2 phase calculated by eq. (2)	
	Monoclinic wt. (%)	Tetragonal wt. (%)	Monoclinic wt. (%)	Tetragonal wt. (%)
0	15.72	84.28	26.03	73.97
0.5	15.73	84.27	13.22	86.78
1	16.76	83.24	15.18	84.82
1.5	16.33	83.67	14.26	85.74
2	15.72	84.28	13.48	86.52
2.5	19.06	80.94	16.37	83.63
3	15.07	84.93	15.24	84.76
4	16.85	83.15	15.01	84.99
5	17.20	82.80	16.53	83.47
10	20.57	79.43	19.42	80.58

Apart from the changes in diffraction intensities as shown in Figure 2, the t (111) peak shift was also observed when various milling times were employed. It was found that t (111) peak of the sample milled for 1.5 h is shifted to higher diffraction angle compared with unmilled, 0.5 and 1 h milled samples (*i.e.* from $2\theta \sim 30.25°$ to 30.50°). However, the t (111) peaks of the other samples, milled for 2 h to 10 h, were shifted back to lower diffraction angles continuously when the milling time was progressively increased. The shifting for the (*hkl*) peaks with a high value of 2θ may be due to experimental errors of XRD technique such as the displacement of the specimen [27]. Furthermore, the progressive shift of the t (111) peak to lower value of 2θ may show the crystal structure changes, or lattice distortion of the substance (*i.e.* tetragonal to monoclinic), in agreement with Muslimin *et al.* [28] and Devi *et al.* [29].

Moreover, with longer milling time, t (111) peak-broadening, an indication of a continuous decrease of crystallite size and of the introduction of lattice strain induced by mechanical impacts, was detected as shown in Figure 2, in agreement with Duran *et al.* [30]. These results pointed out that the particle size affects the crystallinity evolution of the phase formed by prolonged vibro-milling as shown in Figure 3. These demonstrate that crystallite sizes of all powders are in nanosized range and decrease with increasing of milling times whilst an increase of lattice strain in the milled powders because of the fracture of particles was predated. For ZrO_2 powders, the longer the vibro-milling time, the finer is the particle size, up to a certain level (Table 2). This finding indicated that the steady state of the vibro-milling was attained at ≤ 5 h of milling. In addition, the mean crystallite size is close to ≤ 26 nm. Also, the relative intensities of the Bragg peaks, the variation of t (002) and t (200) peaks splitting seem to be observed from XRD patterns. Zooming in these regions around 2θ of 31° to 37° could clarify this detailed alteration as presented in Figure 4. The results indicate that, with increasing stress by increasing the milling time as mentioned above, the intensity of the t (002) increases, while that of the t (200) simultaneously decreases [31]. These findings certainly affect the tetragonality ($c_{(002)}/a_{(200)}$) factors of the tetragonal ZrO_2 phase. The estimated c/a

values for all samples are given in Table 2. It was found that the *c*/*a* ratio is likely to be independent of milling time from 0 to 3 h. However, when increasing the milling time more than 3 h, the results show that the *c*/*a* ratio tends to decrease continuously. It is known that the *c*/*a* ratio is the factor of the tetragonal ZrO_2 phase. Thus, it may be concluded that decreasing of *c*/*a* ratio is associated with (t) to (m) phase transformation causing many stresses and strains to be included in the structure, in agreement with earlier work [27]. Now, it can be summarized that different vibro-milling times affect the phase transformation behavior of ZrO_2 powders and therefore affect other values analyzed from XRD results especially crystallite size. Although these results indicate a continuous decreasing of crystallite size for milled powders as the milling time was increased, it is well-documented that, Sherrer's analysis providing crystallite size can be under estimation, making it almost impossible to obtain reliable particle size information solely from XRD [32]. Therefore, particle size distribution, SEM and TEM techniques were employed to further examine these ZrO_2 powders.

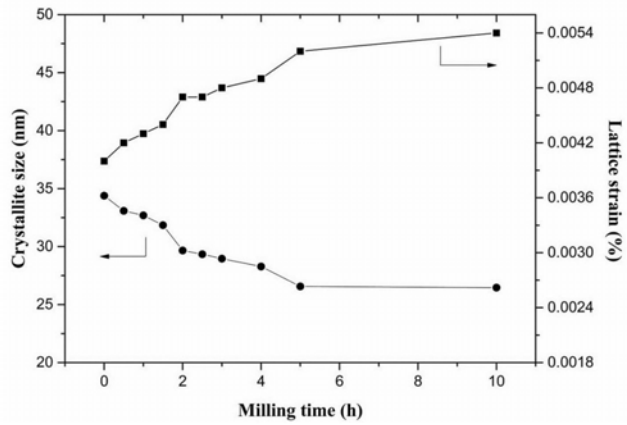

Figure 3. Variation of crystallite size and lattice strain of ZrO_2 powders as a function of milling times.

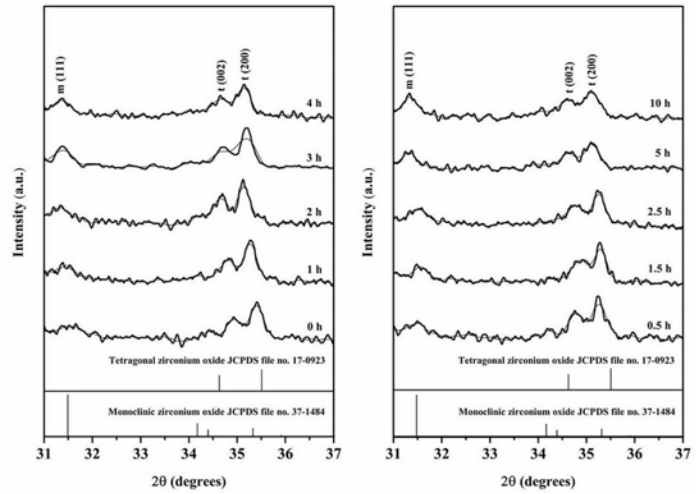

Figure 4. Enlarged zone of Figure 1 showing relative ratios of the t (002) / t (200) peaks as a function of milling time.

Table 2. Effect of milling time on the variation of lattice stain and particle size of waste ZrO_2 powders measured by different techniques.

Milling time (h)	Technique	XRD			Laser scattering		SEM		TEM		Ref.
		A (± 0.05 nm)	$c_{(012)}/a_{(200)}$ (± 0.05 nm)	Lattice strain	D (μm)	P (μm)	D (nm)	P (nm)	D (nm)	P (nm)	
As-received	vibro-milling	34.39	1.01331	0.0040	36.17	1.53-74.03	147.29	87.62-159.01	85.50	64.69-101.94	this work
0.5		33.08	1.01333	0.0042	24.06	0.67-49.75	137.82	84.37-153.61	85.06	61.50-124.32	
1		32.69	1.01318	0.0043	21.15	0.55-46.04	126.58	75.12-127.08	84.53	61.18-96.54	
1.5		31.85	1.01314	0.0044	15.13	0.61-33.24	99.31	68.34-118.93	84.25	60.75-100.91	
2		29.66	1.01331	0.0047	13.58	0.41-28.92	94.13	35.38-133.13	83.63	60.05-106.46	
2.5		29.34	1.01249	0.0047	9.79	0.27-21.11	88.89	58.48-138.61	75.69	51.54-101.91	
3		28.96	1.01309	0.0048	7.23	0.27-16.69	86.80	59.01-135.20	70.49	50.94-105.54	
4		28.28	1.01308	0.0049	6.09	0.23-13.41	79.83	47.57-206.21	69.03	46.40-91.62	
5		26.57	1.01303	0.0052	4.48	0.21-10.49	72.03	47.02-186.34	66.23	43.01-85.93	
10		26.46	1.01248	0.0054	3.22	0.24-8.02	64.36	46.68-194.30	64.53	38.36-94.40	[34]
As-received	High energy ball-milling	281	-	-	281	-	-	200.00-500.00	-	-	
10		50	-	-	65	-	-	> 500	-	-	
15		34	-	-	44	-	-	> 100	-	-	
20		29	-	-	39	-	-	-	-	-	

The effect of milling time on particle size distribution of ZrO_2 powders was also found to be quite significant, as shown in Figure 5 and Table 2. At 0 h milling time, it can be clearly seen that particle size distribution curve separates into two groups (peaks). First group is the particle size ranging from 0.05 to 3.34 μm, while the second group is in the range of 3.34 to 150 μm. When increasing milling times from 0.5 to 4 h, the powders were observed to have a similar type of particle size distribution as trimodal distribution. Compared with previous bimodal curve of 0 h milled powders, additional peak observed from these trimodal curves is found in the range of 0.63 to 3.34 μm. This additional peak is believed to arise mainly from a decrease of primary particle size (observed from main peak). Possible explanation for this finding is the interaction of the particles during milling between the frictional and the impact forces due to higher frequency of collision from the cylindrical grinding. Moreover, more broadening of particle size distribution was found after prolonged milling which is a typical behavior of the high-energy milling process. In addition, it was observed that the main peak was significantly shifted to smaller-size region after prolonged milling time. These results can indicate that vibro-milling technique is the potential method to reduce the particle sizes of ZrO_2 powders.

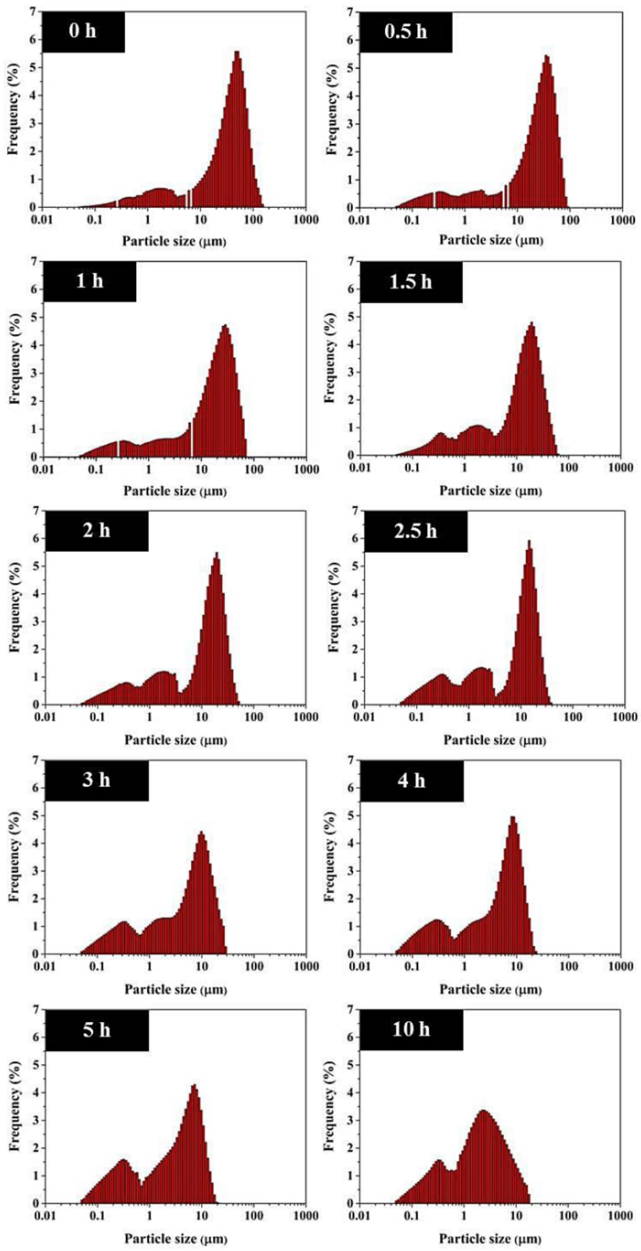

Figure 5. Particle size distributions of waste ZrO_2 powders milled for different time.

It is well-known that the particle size of powders significantly influences consolidated compact to high densities and reduce microstructure defects in the sintered ceramics [33]. Ideally, in order to fabricate a dense and uniform microstructure at a given sintering temperature, fine powders with a minimal level of particle agglomeration are required. Therefore, the influence of agglomerates on powder packing efficiency is significant and has been an important subject of considerable interest in order to select the optimal condition for producing the ZrO_2 powders, and morphological study is also necessary. In connection with this, simple microscopy (SEM and TEM) techniques were conducted

for particle morphology (size and shape) identification, as details listed in Table 2. The morphological evolution of ZrO_2 powders milled with different time was also revealed (Figures 6 and 7). Obviously, the morphological characteristic of as-received dental ZrO_2-based pre-sinter block powders (0 h milling) is similar to other samples. In general, agglomerated and typically irregular in shape, with a significant fluctuation in particle size were found. The powders consist of primary particles with nanometer scale in diameter. When increasing the milling time over the range 0.5 to 10 h, the average size of the ZrO_2 particles tend to decrease significantly, as listed in Table 2. In this work, larger particle sizes obtained for a milling time longer than 2 h could be attributed to the surface energy reduction mechanism of the powders, *i.e.* the smaller the size the higher the specific surface area [34]. It is seen that longer milling time leads to larger particle sizes and higher degree of agglomeration with hard inter-particle bonds within each aggregate generated resulting from dissipated heat energy of prolong milling process [35]. More equiaxed particle's shape seems to be revealed at longer vibro-milling times (Figure 6). At the same time, smaller particle size is revealed and fracture is considered to be the major mechanism at long milling times. In this work, the optimal milling time for the production of ZrO_2 powders with nanosize from dental ZrO_2-based pre-sinter block debris seems to be 2 h because this condition seems to provide the lowest agglomeration with a narrow particle size distribution and soft agglomeration.

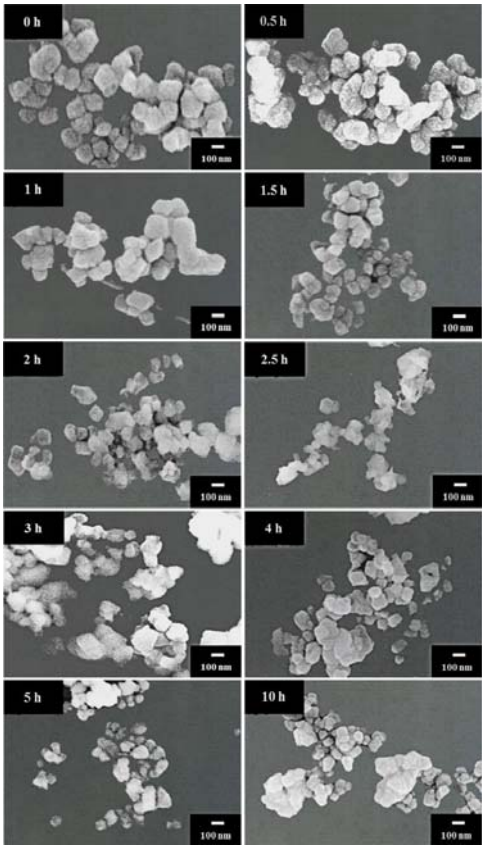

Figure 6. SEM images of waste ZrO_2 powders milled for different time.

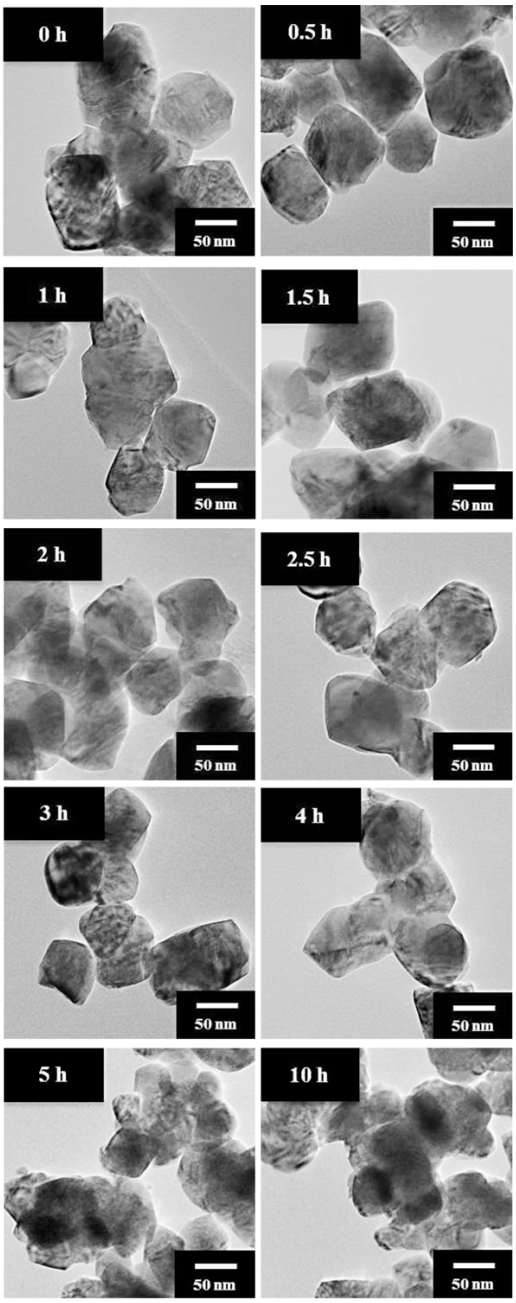

Figure 7. TEM images of waste ZrO_2 powders milled for different time.

Bright field TEM image of typical nanoparticle of the ZrO_2 powder derived from milling time of 2 h was taken and shown in Figure 8 (*center*). By employing the selected area electron diffraction (SAED) technique, it was predicted that two co-existing phases of the monoclinic- and the tetragonal-ZrO_2 phases might be observed from the presence of darker and brighter areas (Figure 8(*i*-a) and (*i*-b), respectively) in a selected particle. To prove this assumption, the reciprocal lattice patterns were simulated with the Carine Crytallography 3.0 software, as presented both in Figure 8 (*ii*-a) and (*ii*-b), respectively. It was found that the SAED patterns recorded from the darker and brighter areas could be indexed as the (t) ZrO_2 and (m) ZrO_2 phases, respectively, in agreement with the XRD results. The advantage of TEM in identifying the presence of nanoparticles in these samples is evidenced, which were otherwise hardly observed due to the limitation of SEM technique [36].

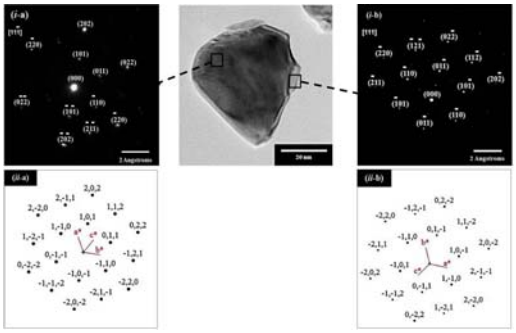

Figure 8. TEM bright image of waste ZrO_2 nanoparticles milled for 2 h (*center*), SAED patterns (*i*) of the major phase of tetragonal ZrO_2 (zone axes [11$\bar{1}$]) (a) and the minor phase of monoclinic ZrO_2 (zone axes [111]) (b) together with the reciprocal lattice pattern simulation of the ZrO_2 phases (*ii*).

Table 2 also exhibited the average particle size of ZrO_2 particles derived from this present work compared with other work [34]. It was found that the average particle size milled by using ball-milling technique is larger than that using vibro-milling technique at the same period (10 h). This may be due to

different impact energy between ball-to-ball, ball-to-powder and ball-to-inner wall in jar of each method. It demonstrated that vibro-milling time operation is the potential method to reduce the particle sizes of ZrO_2 nanopowders. From this study, a strong relationship between the vibro-milling time and a partial re-agglomeration of ZrO_2 nanoparticles was found and 2 h milling time was selected as the optimal condition for the production of nanosized ZrO_2 powder. In addition, in case of the vibro-milling process, other parameters such as the milling speed, milling scale and type of milling media also need to be taken into account for further work.

4. CONCLUSIONS

This work demonstrated that ZrO_2 nanopowders can be successfully produced from dental ZrO_2-based pre-sinter block debris by applying an appropriate choice of vibro-milling time. A combination of XRD, laser diffraction scattering, SEM and TEM techniques was employed to investigate the influence of milling time (ranging from 0 to 10 h) on phase identification, crystallite size, particle distribution, particle size and morphology of ZrO_2 nanopowders. All conditions could provide nanopowders with tetragonal ZrO_2 as a major phase and monoclinic ZrO_2 as a minor phase where the sample milling for 2 h provided the minimum degree of particle agglomeration and be considered as the optimal condition found for the present work.

ACKNOWLEDGEMENTS

This work was supported by the National Research University Project under Thailand's Office of the Higher Education Commission, the Thailand Research Fund IRG5780013 and the Graduate School, Chiang Mai University.

REFERENCES

[1] Pittayachawan P., McDonald A., Young A. and Knowles J.C., *J. Biomed. Mater. Res., Part B*, 2009; **88B**: 366-377. DOI 10.1002/jbm.b.31064.

[2] Manicone P.F., Iommetti P.R. and Raffaelli L., *J. Dent.,* 2007; **35**: 819-826. DOI 10.1016/j.jdent.2007.07.008.

[3] Kosmać T., Dakskobler A., Oblak E. and Jevnikar P., *Int. J. Appl. Ceram. Technol.,* 2007; **4**: 164-174. DOI 10.1111/j.1744-7402.2007.02124.x.

[4] Moldovan O., Luthardt R.G., Corcodel N. and Rudolph H., *Dent. Mater.,* 2011; **27**: 1273-1278. DOI 10.1016/j.dental.2011.09.006.

[5] Elgayar I. and Aboushelib M.N., *Int. J. Chem. Appl. Biol. Sci.,* 2014; **1**: S132-S134. DOI 10.4103/2348-0734.146957.

[6] Kojima T., Mori Y., Kamiya M., Sasai R. and Itoh H., *J. Mater. Sci.*, 2007; **42**: 6056-6061. DOI 10.1007/s10853-006-1167-4.

[7] Kamiya M., Mori Y., Kojima T., Sasai R. and Itoh H., *J. Mater. Cycles Waste Manag.*, 2007; **9**: 27-33. DOI 10.1007/s10163-006-0168-3.

[8] Piconi C. and Maccauro G., *Biomaterials*, 1999; **20**: 1-25. DOI 10.1016/S0142-9612(98)00010-6.

[9] Khamman O., Wongmaneerung R., Chaisan W., Yimnirun R. and Ananta S., *J. Alloys Compd.,* 2008; **456**: 492-497. DOI 10.1016/j.jallcom.2007.02.109.

[10] Wongmaneerung R., Chaisan W., Khamman O., Yimnirun R. and Ananta S., *Ceram. Int.,* 2008; **34**: 813-817. DOI 10.1016/j.ceramint.2007.09.090.

[11] Dabhade V.V., Mohan T.R.R. and Ramakrishnan P., *Appl. Surf. Sci.,* 2001; **182**: 390-393. DOI 10.1016/S0169-4332(01)00456-1.

[12] Cullity B.D., *Elements of X-ray Diffraction*, 2nd Edn., Addison-Wesley Publishing Company, Massachusetts, 1978.

[13] Klug H.P. and Alexander L.E., *X-ray Diffraction Procedures for Polycrystalline and Amorphous Materials*, 2nd Edn., John Wiley and Sons, New York, 1954.

[14] Garvie R.C., *J. Phys. Chem.,* 1978; **82**: 218-224. DOI 10.1021/j100491a016.

[15] Garvie R.C., *J. Phys. Chem.,* 1965; **69**: 1238-1243. DOI 10.1021/j100888a024.

[16] Bailey J.E., Librant Z.M., Lewis D. and Porter L.J., *Trans. J. Br. Ceram. Soc.*, 1972; **71**: 25-30.

[17] Whitney E.D., *Trans. Faraday Soc.,* 1965; **61**: 1991-2000. DOI 10.1039/TF9656101991.

[18] Mitsuhashi T., Ichihara M. and Tatsuke U., *J. Am. Ceram. Soc.,* 1974; **57**: 97-101. DOI 10.1111/j.1151-2916.1974.tb10823.x.

[19] Adam J., Drumm R., Klein G. and Veith M., *J. Am. Ceram. Soc.,* 2008; **91**: 2836-2843. DOI 10.1111/j.1551-2916.2008.02579.x.

[20] Tipakontitikul R. and Ananta S., *Mater. Lett.,* 2004; **58**: 449-454. DOI 10.1016/S0167-577X(03)00523-8.

[21] Murase Y. and Kato E., *J. Am. Ceram. Soc.,* 1979; **62**: 527. DOI 10.1111/j.1151-2916.1979.tb19121.x.

[22] Ananta S. and Thomas N.W., *J. Eur. Ceram. Soc.,* 1999; **19**: 155-163. DOI 10.1016/S0955-2219(98)00194-0.

[23] Toraya H., Yoshimura M. and Somiya S., *J. Am. Ceram. Soc.,* 1984; **67**: C-119-C-121. DOI 10.1111/j.1151-2916.1984.tb19715.x.

[24] Schmid H.K., *J. Am. Ceram. Soc.,* 1987; **70**: 367-376. DOI 10.1111/j.1151-2916.1987.tb05009.x.

[25] Zakeri M., Razavi M., Rahimipour M.R. and Abbasi B.J., *Phys. B*, 2014; **444**: 49-53. DOI 10.1016/j.physb.2014.03.010.

[26] Shukla S., Seal S., Vij R., Bandyopadhyay S. and Rahman Z., *Nano Lett.*, 2002; **2**: 989-993. DOI 10.1021/nl025660b.

[27] Luo J. and Stevens R., *J. Am. Ceram. Soc.,* 1999; **82**: 1922-1924. DOI 10.1111/j.1151-2916.1999.tb02017.x.

[28] Muslimin M. and Sulaiman M.Y.M., *J. Nucl. Relat. Technol.,* 2009; **6**: 95-102.

[29] Devi S. and Jha A.K., *Int. J. Mod. Phys. Conf. Ser.,* 2013; **22**: 140-147. DOI 10.1142/S2010194513010027.

[30] Duran C., Sato K., Hotta Y., Gocmez H. and Watari K., *Ceram. Int.,* 2015; **41**: 5588-5593. DOI 10.1016/j.ceramint.2014.12.138.

[31] Jue J.F. and Virkar A.V., *J. Am. Ceram. Soc.,* 1990; **73**: 3650-3657. DOI 10.1111/j.1151-2916.1990.tb04271.x.

[32] Suryanarayana C., *Prog. Mater. Sci.*, 2001; **46**: 1-184. DOI 10.1016/S0079-6425(99)00010-9.

[33] Liu D.M., Lin J.T. and Tuan W.H., *Ceram. Int.*, 1999; **25**: 551-559. DOI 10.1016/S0272-8842(97)00094-1.

[34] Goyal R.K., Deshpande S.P. and Singare S.S., *J. Mater. Sci. Surf. Eng.*, 2016; **4**: 360-363.

[35] Wongmaneerung R., Yimnirun R. and Ananta S., *Mater. Lett.,* 2006; **60**: 1447-1452. DOI 10.1016/j.matlet.2005.11.043.

[36] Rujiwatra A., Tapala S., Luachan S., Khamman O. and Ananta S., *Mater. Lett.,* 2006; **60**: 2893-2895. DOI 10.1016/j.matlet.2006.02.010.